[68]Ga-Labeled Oligonucleotides for In Vivo Imaging with PET

Anne Roivainen, PhD[1,2]; Tuula Tolvanen, MSc[1]; Satu Salomäki, MSc[1,3]; Gabor Lendvai, MSc[2]; Irina Velikyan, MSc[2,4]; Petri Numminen, MSc[1]; Maria Välilä, MSc[1,3]; Hannu Sipilä, MSc[1]; Mats Bergström, PhD[2]; Pirkko Härkönen, MD, PhD[5]; Harri Lönnberg, PhD[3]; and Bengt Långström, PhD[2,4]

[1]Turku PET Centre, Turku University Hospital, Turku, Finland; [2]Uppsala Imanet, Uppsala, Sweden; [3]Department of Chemistry, University of Turku, Turku, Finland; [4]Department of Organic Chemistry, Institute of Chemistry, Uppsala University, Uppsala, Sweden; [5]Institute of Biomedicine and Medicity Research Laboratory, University of Turku, Turku, Finland

The biologic evaluation in living rats of ^{68}Ga-labeled oligonucleotides as imaging agents for PET is reported. **Methods:** [68]Ga, a positron-emitting radionuclide (half-life, 68 min), along with a macrocyclic chelating agent, 1,4,7,10-tetraaza-cyclododecane-N,N',N'',N'''-tetraacetic acid (DOTA), was used for labeling of antisense oligonucleotides targeting activated human K-ras oncogene. The biologic properties of 3 different forms of the oligonucleotides—that is, 2′-deoxyphosphodiester (PO), 2′-deoxyphosphorothioate (PS), and 2′-O-methyl phosphodiester (OMe)—were studied first. The biodistribution and biokinetics were evaluated in vivo in athymic rats, each bearing a tumor of A549 cells, containing K-ras point mutation in codon 12, and a tumor of BxPC-3 cells, containing wild-type K-ras. Dynamic PET imaging lasting up to 2 h was performed immediately after intravenous injection of ^{68}Ga-oligonucleotide. Blank studies were performed using [68]GaCl$_3$ or ^{68}Ga-DOTA alone without oligonucleotide. The ^{68}Ga-antisense oligonucleotide uptake in tumors was also compared with the ^{18}F-FDG and ^{68}Ga-sense oligonucleotide uptakes. In addition, oligonucleotide binding to human plasma proteins and to human albumin was examined by means of ultrafiltration. **Results:** The oligonucleotides can be stably labeled with ^{68}Ga and DOTA chelate. Intravenously injected ^{68}Ga-oligonucleotides of 17-mer length revealed high-quality PET images, allowing quantification of the biokinetics in major organs and in tumors. The biodistribution and biokinetics of intravenously administered ^{68}Ga-oligonucleotide varied considerably with the nature of the oligonucleotide backbone. **Conclusion:** We conclude that ^{68}Ga labeling of oligonucleotides is a convenient approach for in vivo imaging and quantification of oligonucleotide biokinetics in living animals with PET.

Key Words: [68]Ga; oligonucleotides; in vivo imaging; PET; biokinetics

J Nucl Med 2004; 45:347–355

At the moment, in vivo imaging of genes is still in its infancy (1–4). Several methods that describe the labeling of antisense oligonucleotides with positron-emitting isotopes—for example, ^{11}C, ^{18}F, or [76]Br—have been published (5–9). Yet, only a few molecular imaging trials with experimental animals have been described (5,10). The present project focuses on the use of ^{68}Ga-labeled antisense oligonucleotides as tracers for PET imaging, placing special emphasis on the assessment of the biologic parameters of neoplastic tissue. Alterations in the cellular genes, which directly or indirectly control cell growth and differentiation, are generally considered to be the main cause of cancer.

In a development program directed toward in vivo imaging of gene expression using PET, we have chosen K-ras oncogene as a model because of its significance in cancer biology and oncology. The ras oncogene mutations are found in a variety of human tumors but not in normal tissue, which makes ras messenger RNAs (mRNAs) suitable targets for demonstration of gene expression by noninvasive imaging with ^{68}Ga-antisense oligonucleotides. The incidence of K-ras point mutation is extremely high (>80%) in pancreatic carcinomas (11). The sequence of K-ras oncogene is well characterized (12). Monia et al. have tested several antisense oligonucleotides targeted to ras oncogenes (13,14). Selectivity for the activated ras and the binding ability of differently modified oligonucleotides to wild-type versus mutated ras oncogenes have also been examined by others (15–18).

The natural forms of oligonucleotides—that is, 2′-deoxy-phosphodiester (PO)—are unstable in vivo, degrading rapidly by nuclease digestion both intracellularly and in the systemic circulation; the half-life in plasma is about 5 min (19). Considering the nuclease sensitivity of oligonucleotides, several modifications have been explored to find good candidates possessing enhanced permeability, stability, and target affinity. Among various sugar-phosphate backbone modifications, 2′-deoxyphosphorothioate (PS) features a significantly longer half-life (ranging from a few hours to days), thus being available for the biologic target within the

cell (20,21). However, the 2′-O-alkyl modifications, such as 2′-O-methyl phosphodiester (OMe), that are relatively resistant to endo- and exonucleases have a better affinity to the target (22).

In this article we present the in vitro and in vivo characteristics of 3 ^{68}Ga-antisense oligonucleotides—that is, PO, PS, and OMe sequences—specific to human K-ras oncogene activated by point mutation. Knowledge about the development and use of radiolabeled antisense oligonucleotides for in vivo imaging of specific gene targets will be of significance, considering not only the biology of tumors but also the possible applications in designing novel molecule-targeted therapies of cancer.

MATERIALS AND METHODS

^{68}Ga Labeling of Oligonucleotides

The 17-mer PO and PS oligonucleotides bearing a 5′-aminohexyl tether and aimed at targeting codon 12 point mutation of human K-ras oncogene (23) were purchased from Scandinavian Gene Synthesis AB. A similarly derivatized OMe oligoribonucleotide was assembled by the conventional phosphoramidite strategy from the 5′-O-(4,4′-dimethoxytrityl)-2′-O-methylribonucleoside 3′-(2-cyanoethyl-N,N-diisopropylphosphoramidite) building blocks (Glen Research) and purified as described below. According to a GenBank search, the selected sequence did not have any complementary sequence in rat tissue. Oligonucleotides corresponding to the mutation-specific sense sequence were used as controls. Accordingly, the antisense and sense sequences used here were 5′-CTACGC-CACTAGCTCCA-3′ and 5′-TGGAGCTAGTGGCGTAG-3′, respectively.

The amino-tethered 2′-O-methyl phosphodiester oligonucleotide was purified by ion-exchange high-performance liquid chromatography (HPLC) (SynChropak AX300, 250 × 4.6 mm; EiChrom Technologies). HPLC conditions were as follows: A/B gradient, where solution A was KH_2PO_4 (0.05 mol/L, pH = 5.6) in formamide:water (50:50, v/v) and solution B was solution A + $(NH_4)_2SO_4$ (0.6 mol/L). Gradient elution from 10% to 70% B was applied. The product was desalted by reverse-phase (RP) HPLC (Hypersil ODS, 250 × 10 mm, 5 μm; Merck), applying gradient elution from water to 50% (v/v) aqueous acetonitrile. The identity of the oligonucleotide conjugate was verified by mass spectrometry (PE Sciex API 365 Triple Quadrupole LC/ESI-MS/MS; Perkin-Elmer) and by capillary electrophoresis (HP^{3D}CE; Hewlett-Packard).

1,4,7,10-Tetraazacyclododecane-N,N′,N″,N‴-tetraacetic acid (DOTA; Macrocyclics) and N-hydroxysulfosuccinimide (Sulfo-NHS; Fluka Chemie AG) in H_2O were added to 1-ethyl-3-(3-dimethylaminopropyl)carbodiimide (Sigma Chemical Co.) in H_2O and kept on ice for 30 min and then warmed to room temperature to yield DOTA-Sulfo-NHS (24). The DOTA-NHS-solution was added to the oligonucleotide in carbonate buffer (1 mol/L, pH 9) and cooled on ice. The mixture was left at room temperature for 10 h (25). The reaction mixture was sequencially purified through NAP5 (Sephadex G-25; Amersham Pharmacia Biotech AB) and C_{18} solid-phase extraction (SPE) columns (Supelclean LC-18 SPE tubes; Supelco). The DOTA-oligonucleotide was eluted with acetonitrile:water (50:50, v/v), evaporated, redissolved in water, and stored in 4°C until use.

^{68}Ga was obtained in 0.1 mol/L HCl (1 mL) from a ^{68}Ge/^{68}Ga generator (Cyclotron C; Obninsk), and sodium acetate was added to give pH ~5.5 (26). Then, DOTA-oligonucleotide (10–100 nmol) was added and the mixture was incubated in 100°C for 10 min. The reaction mixture was applied on the C_{18} SPE column, the product was eluted in ethanol:water (50:50, v/v), and the ethanol was evaporated.

The product was analyzed by radio-HPLC using a μBondapak C_{18} column (125Å, 10 μm, 7.8 × 300 mm; Waters); flow: 6.0 mL/min A = 20 mmol/L triethylammonium acetate buffer; B = 100% acetonitrile; C = 50 mmol/L phosphoric acid; linear gradient: 0–3 min A (100%–95%), B (0%–5%); 3–6 min A (95%–90%), B (5%–10%); 6–10 min A (90%–85%), B (10%–15%); 10–15 min A (85%–50%), B (15%–50%); 15–20 min A (50%–0%), B (50%–0%), C (0%–100%); 20–30 min C 100%; λ = 260 nm. The HPLC system consisted of LaChrom Instruments (Hitachi; Merck) and of a Radiomatic 150TR radioisotope detector (Packard).

Protein Binding Assays

The ^{68}Ga-oligonucleotide was spiked at different concentrations to human plasma and incubated at 37°C for 30 min. Subsequently, plasma was transferred to Ultrafree-MC (Millipore) ultracentrifuge inserts (Biomax-30 polysulfone membrane with a nominal molecular weight limit of 30,000) and centrifuged at 12,300g for 20 min, collecting ~20% of the loaded volume in the filtrate. Radioactivity in whole plasma and in the filtrate was measured using a γ-counter (1480 Wizard 3″ γ-Counter; EG&G Wallac). The fraction bound to protein was calculated by subtracting the unbound (filtrate) from 100%.

A fixed amount of ^{68}Ga-oligonucleotide was mixed with increasing concentrations of human albumin (fatty acid-free serum albumin; Sigma Chemical Co.) and incubated for 1 h in phosphate-buffered saline containing 10 mmol/L ethylenediaminetetraacetic acid (EDTA) and 0.005% Tween 80. Blank studies were performed using ^{68}GaCl$_3$ or ^{68}Ga-DOTA alone without oligonucleotide. After the incubation, the samples were loaded onto Microcon YM-30 filters (regenerated cellulose membranes with a nominal molecular weight limit of 30,000; Millipore) and centrifuged at 9,500g for 10 min. Radioactivity was measured from both the filtrate and the unfiltered solutions, and the amount of oligonucleotide bound to albumin was calculated as described above.

Hybridization in Solution

The ^{68}Ga-antisense oligonucleotide (PO, PS, and OMe) in 50% ethanol was evaporated and dissolved in TES buffer (50 mmol/L Tris, pH 8.0, 50 mmol/L NaCl, 1 mmol/L EDTA). The hybridization mixture was prepared as follows: A gradually increased concentration of PO sense oligonucleotide (0.33–80 pmol) was added to a constant concentration of ^{68}Ga-oligonucleotide (20 pmol), and the total volume was adjusted to 10 μL with TES buffer. As reference solutions, 40 pmol of ^{68}Ga-oligonucleotide or unlabeled PO sense oligonucleotide were used. All mixtures were kept on ice until hybridization at 40°C for 10 min. Subsequently, samples were run on a 20% polyacrylamide gel electrophoresis (PAGE) gel along with a molecular weight marker. After electrophoresis, the gel was stained using ethidium bromide and photographed under ultraviolet light. Then, the gel was exposed to a phosphor imaging plate for 12 h, scanned using a Phosphorimager SI device, and analyzed using Image Quant 5.1 software (Molecular Dynamics Inc.).

RT-PCR and PCR

The mRNA and genomic DNA were isolated from A549 tumor cells bearing point mutated K-ras gene. The mRNA was converted into single- strand complementary DNA (cDNA) by a sequence of reverse transcription (RT) reaction and polymerase chain reaction (PCR), using a RobusT I RT-PCR kit, which is based on avian myeloblastosis virus reverse transcriptase (AMV-RT) in the first-strand cDNA synthesis and on DyNAzyme EXT DNA polymerase in the second-strand synthesis (Finnzymes Oy). Unlabeled, DOTA-conjugated, or ^{68}Ga-oligonucleotides were used as reverse primers. The sequence of the forward primer (Pr1) was 5′-GACT-GAATATAAACTTGTGG-3′. In a control reaction, the reverse primer (Pr2) had a sequence of 5′-CTATTGTTGGATCATAT-TCG-3′, allowing amplification of a 108-base-pair (bp) PCR product around codon 12 of human K-ras oncogene as described earlier (27). The protocol for RT-PCR amplification was as follows: 40 min at 48°C followed by 2 min at 94°C (1 cycle); denaturing at 94°C for 1 min followed by annealing at 52°C for 1 min and extension at 72°C for 1 min (35 cycles); and final extension at 72°C for 5 min. The DNA samples underwent 40 cycles of PCR: 1 min at 94°C, 1 min at 52°C, and 1 min at 72°C.

The PCR products were run on a 10% PAGE gel along with a molecular weight marker. The DNA bands were visualized with ethidium bromide and photographed under ultraviolet light.

Nuclease Stability

The ^{68}Ga-oligonucleotide was mixed with heparinized human blood and incubated for 5, 30, 60, or 120 min at 37°C. Plasma retained after centrifugation was filtered through Microcon YM-30 filters for the separation of proteins and analyzed by radio-HPLC as described above.

Tumor Model

Two human tumor cell lines—that is, A549 lung carcinoma cell line harboring codon 12 mutated K-ras oncogene and BxPC-3 pancreatic adenocarcinoma cell line harboring wild-type K-ras—were purchased from American Type Culture Collection and grown in RPMI 1640 medium containing 10% fetal bovine serum without antibiotics. Male athymic Hsd:RH-rnu/rnu rats were obtained from Harlan, Netherlands, at the age of 6 wk and kept in the Central Animal Laboratory of the University of Turku in filter-top cages and allowed food and water ad libitum. Tumor cells (10^7 per rat) were injected subcutaneously into the flank region, and tumors were allowed to grow to a size of 1–2 cm in diameter. All animal studies were approved by the local University Laboratory Animal Committee.

Dynamic PET Studies

For PET imaging, rats weighing 353 ± 44 g were anesthetized with intraperitoneal. injection of pentobarbital (60 mg/kg; Mebunat Vet, Orion). PET studies were performed with an Advance PET scanner (General Electric Medical Systems) operated in 2-dimensional mode. The scanner has 18 rings of bismuth germanate detectors and the axial length of the imaging field of view (FOV) is 152 mm. All 35 transaxial image slides were reconstructed with an ordered subsets expectation maximization algorithm and the central 200-mm-diameter transaxial FOV was used. the image pixel size was 1.56 × 1.56 mm in a 128 × 128 matrix. Scatter correction, random counts, and dead time corrections were all incorporated into the reconstruction algorithm. Radiation attenuation in each animal was measured with 2 rotating rod sources containing [68]Ge/^{68}Ga before tracer injection, and the images were corrected for radiation attenuation.

All PET studies started with an 8-min transmission scan. The tracer was injected intravenously via the tail vein as a bolus. The median dose was 11.49 ± 4.52 MBq. The dynamic scanning started immediately after injection. The acquisition times were as follows: 6 × 10 s, 4 × 60 s, and 23 × 300 s (duration, 120 min).

Regions of interest were drawn on major organs and on the tumors. Pharmacokinetic curves, representing the radioactivity concentrations (percentage of injected dose per gram of tissue = %ID/g), versus time after injection were determined accordingly.

Metabolite Analysis

Immediately after PET imaging, blood was obtained by cardiac puncture, followed by an intracardial pentobarbital injection for killing each animal. Subsequently, urine was obtained directly from urinary bladder. Both plasma retained after centrifugation and urine were filtered through Microcon YM-30 filters by centrifugation at 9,500g for 10 min for the separation of proteins. Filtrates were analyzed by radio-HPLC as described above.

Organ Distribution

Samples of blood, urine, tumors, heart, lung, liver, kidney, pancreas, spleen, intestine, adrenal, urinary bladder, testis, brain, muscle, bone, bone marrow, skin, and parotid gland were excised, weighed, and measured in a calibrated γ-counter for 30 s (1480 Wizard 3″ γ-Counter). The radioactivity concentration was expressed as standardized uptake value ([organ activity/organ weight]/[total given radioactivity/rat body weight]).

RESULTS

[68]Ga Labeling of Oligonucleotides

The ^{68}Ga labeling of oligonucleotides is straightforward and applicable to any sequence and oligonucleotide chemistry. The ^{68}Ga-labeling method was originally developed at Uppsala PET Centre and the Department of Organic Chemistry of Uppsala University, Sweden, and later set up at Turku PET Centre, Finland. According to our experience, the method is easily transferable from one laboratory to another and requires only minor investments, the generator being the most expensive acquisition.

In the present study, the reaction of [68]GaCl$_3$ with DOTA-conjugated oligonucleotide was rapid—that is, 10 min at 100°C. In general, 25 MBq of purified ^{68}Ga-oligonucleotide were obtained from 100 MBq of [68]GaCl$_3$ and 55 nmol of DOTA-conjugated oligonucleotide in 30 min with 95%–99% radiochemical purity. The specific activity of ^{68}Ga-oligonucleotide was 270 ± 90 MBq/mg. According to the radio-HPLC analysis, free ^{68}Ga and its DOTA chelate were the main impurities, both present at a very low concentration. The ^{68}Ga-oligonucleotide remained stable in H$_2$O at room temperature for >4 h as demonstrated by repeated radio-HPLC analyses (data not shown).

Biologic Properties of ^{68}Ga-Oligonucleotides

The ability of ^{68}Ga-oligonucleotides to hybridize with a complementary sequence was investigated in a cell-free approach. Our results revealed that ^{68}Ga labeling of oligonucleotides did not alter their hybridization properties. In-

stead, the hybridization of ^{68}Ga-oligonucleotides with a PO sense oligonucleotide of the same length was concentration dependent (Fig. 1). The stained PAGE gels showed that all 3 ^{68}Ga-oligonucleotides (PO, PS, and OMe) were able to hybridize. The hybrid formation increased proportionally with the concentration of sense oligonucleotide.

Interestingly, only PO worked as a reverse primer both in RT-PCR and in PCR reactions. This property was retained after conjugation with DOTA and also after labeling with ^{68}Ga, as shown in Figure 2. No amplification with PS or OMe was observed in either case.

The binding of ^{68}Ga-oligonucleotides to human plasma proteins was studied using the ultrafiltration method. Bind-
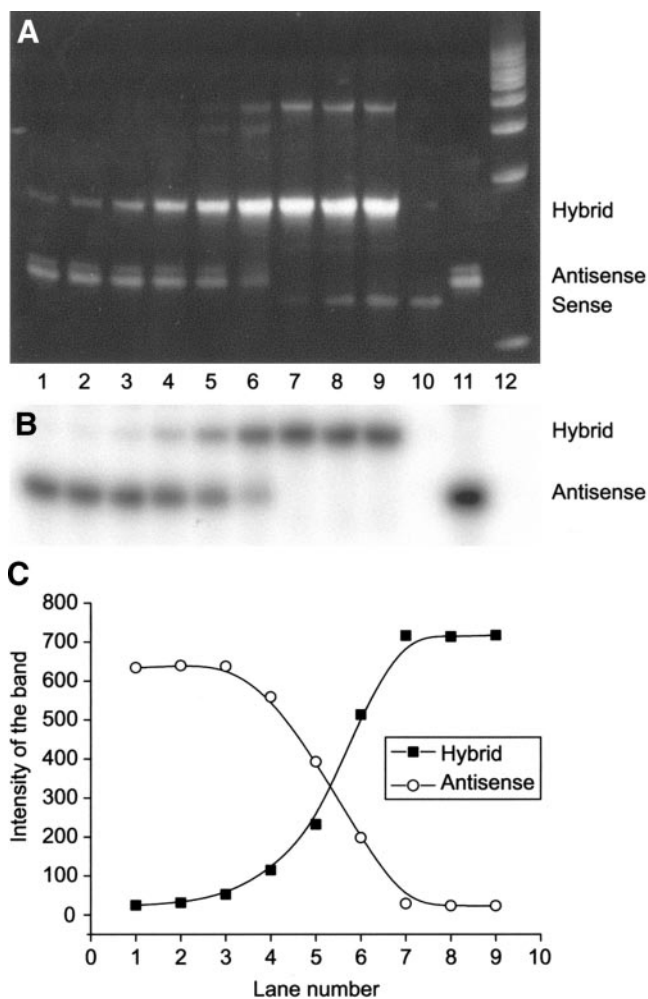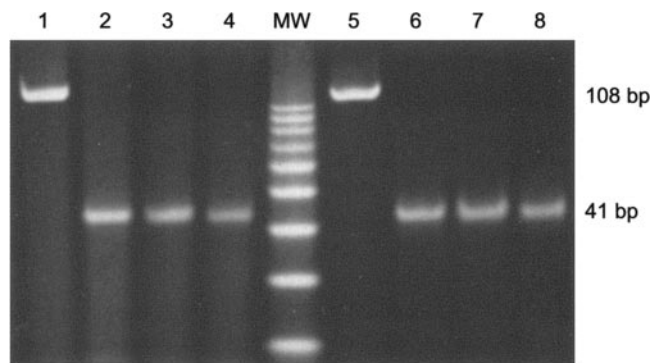
PCR template: genomic DNA from A549 tumor cells
1. Primers: Pr1 + Pr2
2. Primers: Pr1 + PO oligonucleotide
3. Primers: Pr1 + DOTA-conjugated PO oligonucleotide
4. Primers: Pr1 + ^{68}Ga-labeled PO oligonucleotide

RT-PCR template: mRNA from A549 tumor cells
5. Primers: Pr1 + Pr2
6. Primers: Pr1 + PO oligonucleotide
7. Primers: Pr1 + DOTA-conjugated PO oligonucleotide
8. Primers: Pr1 + ^{68}Ga-labeled PO oligonucleotide

FIGURE 2. Ethidium bromide–stained 10% PAGE gel of the PCR and RT-PCR products, using either unlabeled, DOTA-conjugated, or ^{68}Ga-labeled PO antisense oligonucleotide as a reverse primer. A 41-bp fragment corresponding to the K-ras codon 12 region is seen. The A549 cells (human lung carcinoma) contain K-ras oncogene point mutation in codon 12. MW = molecular weight marker.

FIGURE 1. Hybridization of 17-mer ^{68}Ga-labeled PO anti-sense oligonucleotide with unlabeled PO sense oligonucleotide of the same length in a cell-free approach. Ethidium bromide–stained (A) and autoradiographic (B) images of 20% PAGE gels demonstrate the concentration-dependent hybrid formation (C). The concentration ratios of antisense:sense in the lanes are as follows: lane 1, 1:1/60; lane 2, 1:1/30; lane 3, 1:1/15; lane 4, 1:1/5; lane 5, 1:1/2; lane 6, 1:1; lane 7, 1:2; lane 8, 1:3; lane 9, 1:4, and the references are lane 10, unlabeled PO sense oligo-nucleotide; lane 11, ^{68}Ga-labeled PO antisense oligonucleotide; and lane 12, a molecular weight marker.

ing to human albumin seemed to be dependent of the backbone chemistry; PS was bound to the highest extent, and the binding clearly exhibited saturation (Fig. 3). The percentage of protein binding (10%–20%) for both ^{68}Ga-DOTA and ^{68}GaCl$_3$ was much lower compared with that of labeled oligonucleotides (Fig. 3). Binding to whole plasma
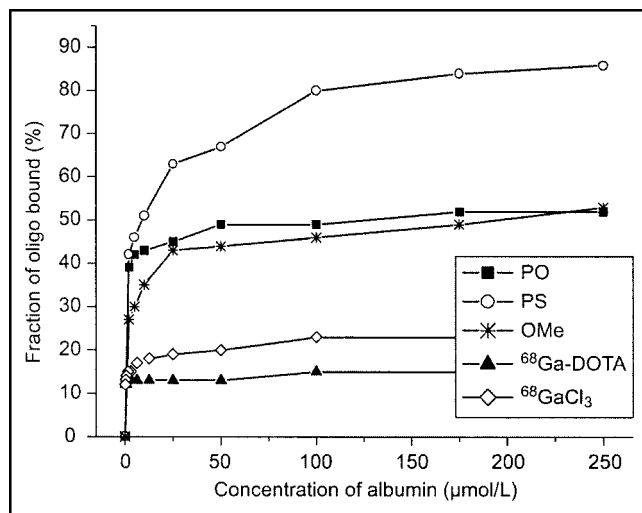
FIGURE 3. Albumin binding of ^{68}Ga-labeled oligonucleotides (oligo). Mean value of 4 experiments ($n = 4$), except for blank studies with ^{68}GaCl$_3$ and ^{68}Ga-DOTA alone without oligonucleotide ($n = 2$).
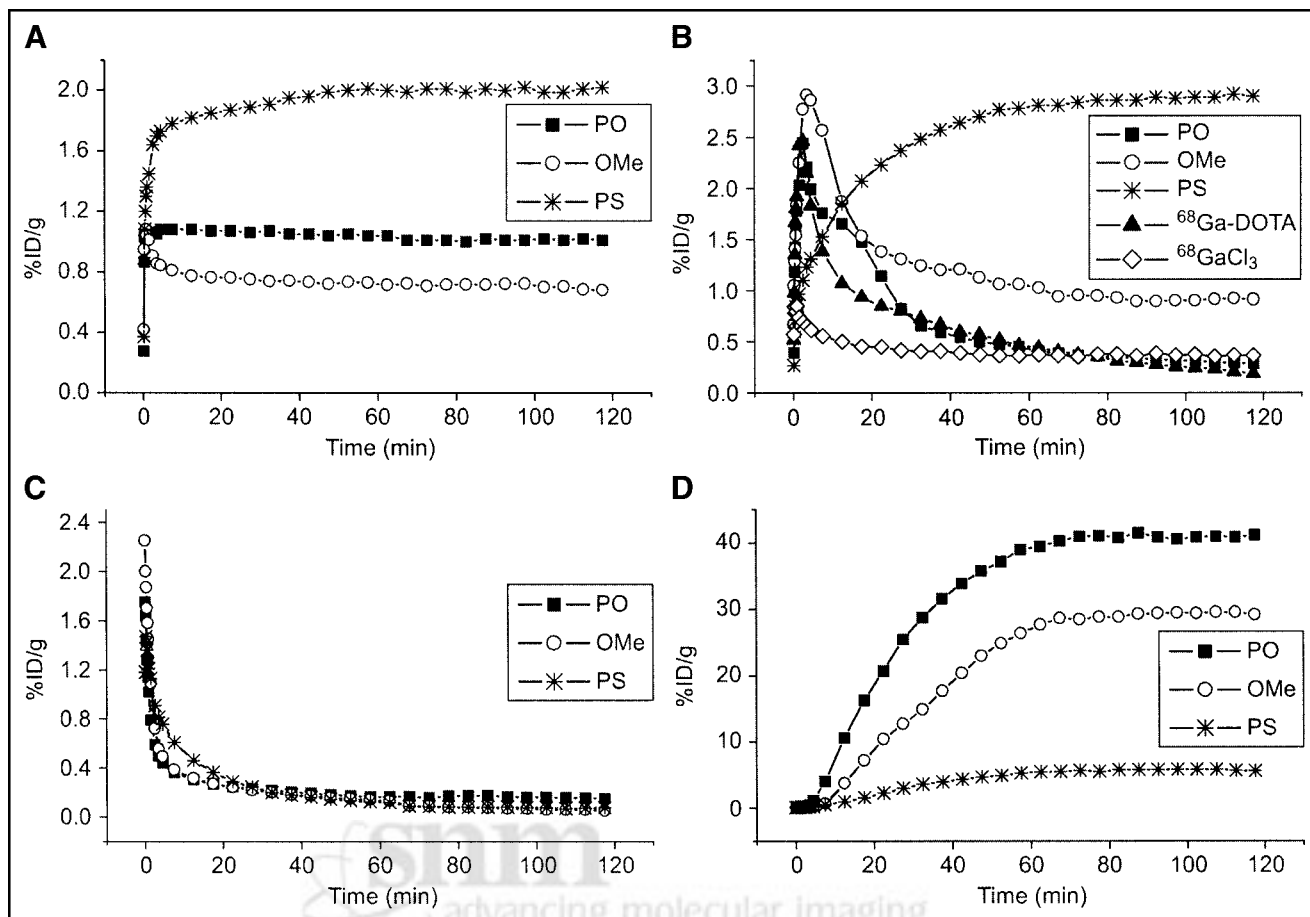
FIGURE 4. In vivo biokinetics (amount of radioactivity vs. time after injection) of intravenously administered 17-mer ^{68}Ga-labeled antisense oligonucleotides specific to codon 12 mutated human K-ras oncogene in rat liver (A), kidney (B), heart (C), and bladder (D). Biokinetics of ^{68}GaCl$_3$ and ^{68}Ga-DOTA without oligonucleotide in rat kidney are also shown. Radioactivity concentrations are expressed as %ID/g of tissue. Mean value of 4–6 rats ($n = 4$–6).

proteins was 99%, 99%, and 96% for PS, OMe, and PO, respectively.

PET Imaging and Quantification of ^{68}Ga-Oligonucleotide Biokinetics in Living Rats

PET imaging was conducted for tumor-bearing rats, using an Advance PET scanner and ^{68}Ga-oligonucleotides with 3 different backbone chemistries. The ^{68}Ga-antisense oligonucleotide uptake in main organs and in tumors was compared with ^{18}F-FDG, ^{68}GaCl$_3$, ^{68}Ga-DOTA, and ^{68}Ga-sense oligonucleotide uptakes. The quantification of biokinetics data—that is, the amount of radioactivity normalized for the injected dose versus time after injection in rat liver, kidney, heart, and bladder—is shown in Figure 4. The biokinetic differences between PO, PS, and OMe are evident.

Tumor Localization of ^{68}Ga-Oligonucleotides

After the last PET imaging, the rats were killed, and tumors, blood, urine, and different organs were excised for the measurement of radioactivity. The tumor-to-blood and tumor-to-muscle ratios were calculated for PO, PS, and OMe (Table 1). Preliminary studies revealed that PS and

OMe localize somewhat better in A549 tumors in contrast to their PO counterpart ($n = 1$–3). The slightly better uptake of PS in an A549 tumor, compared with a BxPC-3 tumor, was observed, as shown in Figures 5 and 6.

TABLE 1
Mean ± SD Values of Tumor-to-Blood and Tumor-to-Muscle Ratios of ^{68}Ga-Labeled Antisense Oligonucleotides Specific to Point Mutated Human K-ras Oncogene

1 h after injection	PO ($n = 2$)	PS ($n = 3$)	OMe ($n = 1$)	^{68}GaCl$_3$ ($n = 1$)
Tumor-to-blood				
BxPC-3 tumor	0.95 ± 0.14	0.80 ± 0.11	0.65	0.34
A549 tumor	0.78 ± 0.09	0.95 ± 0.10	0.68	0.27
Tumor-to-muscle				
BxPC-3 tumor	5.24 ± 0.09	4.92 ± 0.12	3.05	2.36
A549 tumor	4.31 ± 0.08	5.84 ± 0.11	3.17	1.87

BxPC-3 tumor cells were subcutaneously implanted human pancreatic adenocarcinoma cells with wild-type K-ras oncogene; A549 tumor cells were subcutaneously implanted human lung carcinoma cells with point mutated K-ras oncogene.
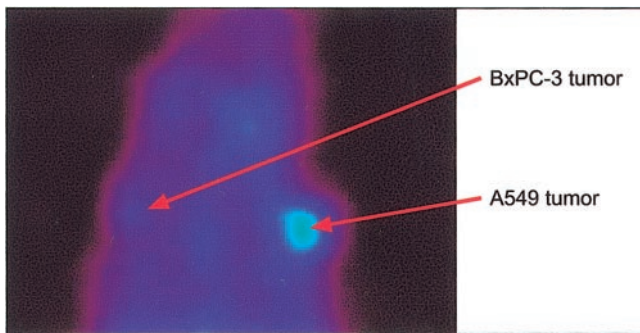
FIGURE 5. PET image of an athymic rat bearing both A549 and BxPC-3 tumors, using ^{68}Ga-labeled PS antisense oligonucleotide specific to codon 12 mutated human K-ras oncogene. The human A549 cells (lung adenocarcinoma) contain K-ras point mutation in codon 12, and the human BxPC-3 cells (pancreatic adenocarcinoma) contain wild-type K-ras oncogene. Image is a summation from 60 to 65 min after injection and is color-coded according to the amount of radioactivity, from dark blue (lowest) to hot red (highest).

In Vivo Stability of ^{68}Ga-Oligonucleotides

Samples of plasma and urine were also subjected to radio-HPLC analysis for the evaluation of in vivo stability of ^{68}Ga-oligonucleotides. Representative radiochromato-
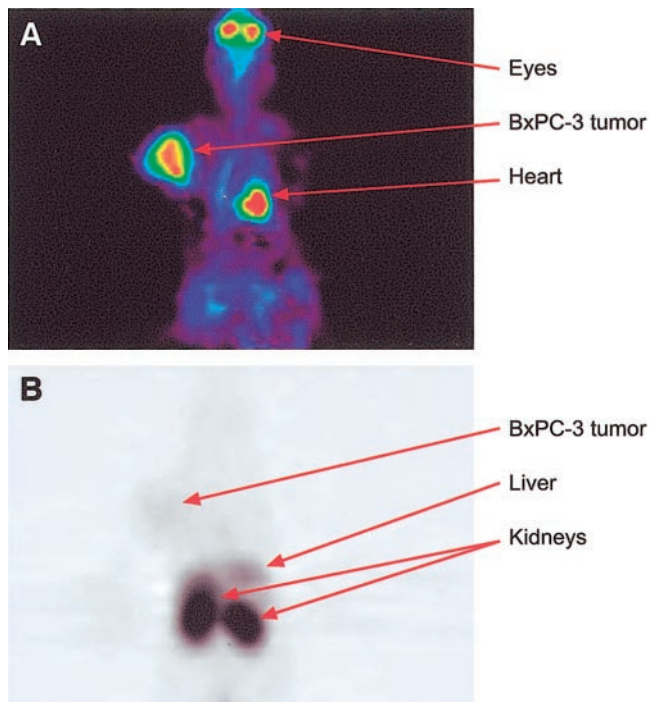

FIGURE 6. Whole-body PET images of a tumor-bearing rat. The animal underwent PET imaging with both ^{18}F-FDG and ^{68}Ga-labeled PS antisense oligonucleotide on separate days. Images are summations from 90- to 95-min follow-up measurements after injection. (A) BxPC-3 tumor (human pancreatic adenocarcinoma) with wild-type K-ras oncogene is clearly visible with ^{18}F-FDG. (B) ^{68}Ga-PS oligonucleotide shows high kidney and liver uptake, compared with low BxPC-3 tumor uptake. Note that this animal did not have an A549 tumor (human lung carcinoma) with point mutated K-ras gene to which the antisense oligonucleotide was specific.

grams are shown in Figure 7. After 120 min, most of the radioactivity in urine derived from free ^{68}Ga-chelate and short 5′-terminal fragments of the probe, not from the intact 17-mer PS oligonucleotide. In plasma filtrate, on the other hand, the PS appeared to be almost intact (Fig. 7B). In contrast, both PO and OMe were totally degraded by nucleases during the 120-min incubation time both in plasma and in urine (data not shown).

DISCUSSION

Antisense oligonucleotides labeled with positron-emitting isotopes ^{11}C, ^{76}Br, and ^{18}F have already been studied as potential PET tracers for molecular imaging (5,7,9). In this study we have used oligonucleotides labeled with generator-
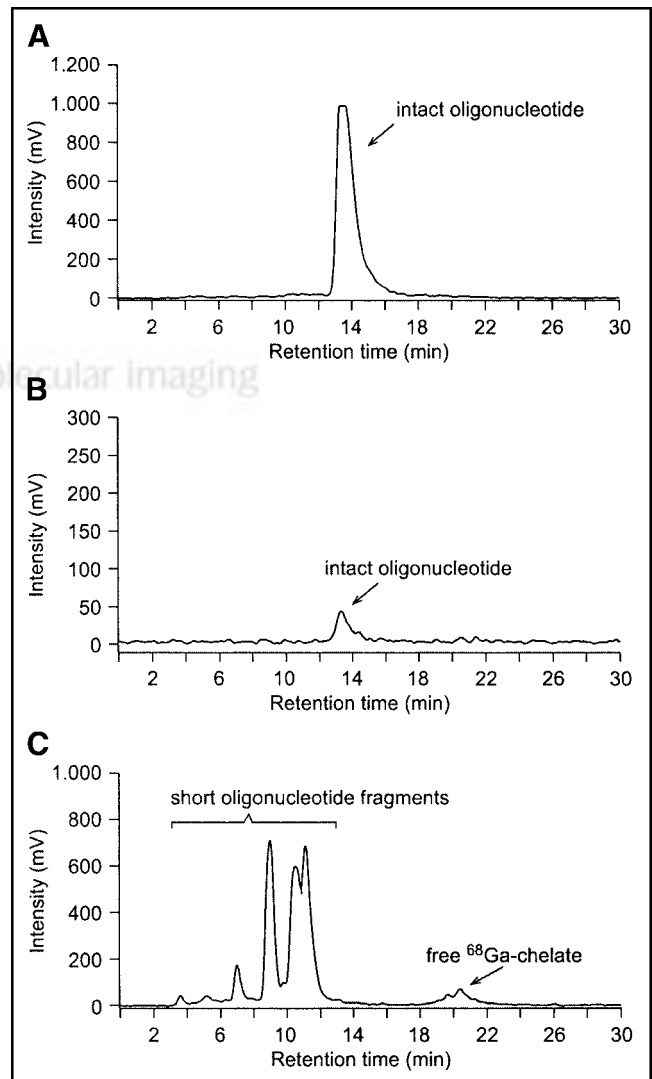

FIGURE 7. Radio-HPLC chromatograms of intact oligonucleotide (A), rat plasma (B), and rat urine (C) taken 120 min after intravenously administered ^{68}Ga-labeled PS oligonucleotide. Most radioactivity in urine derives from free ^{68}Ga-chelate and short oligonucleotide fragments. In plasma, the oligonucleotide appears to be almost intact.

produced ^{68}Ga possessing a sufficiently long half-life (68 min) and appropriate mode of decay (90% β$^+$, 10% electron capture) for PET imaging. With respect to PET imaging, ^{68}Ga has the following advantages over ^{18}F, ^{11}C, or ^{76}Br: (a) The isotope itself is readily available using a low-cost ^{68}Ge/^{68}Ga generator system instead of elaborate and expensive cyclotrons. (b) The half-life is longer than that of ^{11}C (68 min vs. 20 min). (c) The β$^+$ decay energy of ^{68}Ga (90% positrons, 2.921 MeV) is ideal for PET imaging. For comparison, ^{76}Br has a longer half-life (16.2 h) but it decays only 55% by positron emission. Thus, ^{76}Br is suitable for long-lasting in vitro applications, but not for human PET studies. For this study, we investigated the biodistribution and biokinetics of intravenously administered ^{68}Ga-labeled 17-mer PO, PS, and OMe antisense oligonucleotides specific for codon 12 point mutated human K-ras oncogene using tumor-bearing rats.

One of the major challenges in the field of antisense research is the identification of sequences within the target mRNA that would be accessible to an antisense oligonucleotide. Owing to the 3-dimensional folding of mRNA, there are both inaccessible segments and double-stranded regions in the RNA molecule. In addition, for the in vivo applications of antisense oligonucleotides certain hurdles need to be overcome—for example, nuclease resistance, cellular transport and penetration, intracellular distribution, and turnover of the oligonucleotide. Modifications of oligonucleotides to increase their stability must be made without a loss of specificity or hybridization properties. To meet these demands, dozens of structurally modified oligonucleotides have been prepared, but apart from the extensively used PS oligonucleotides (*20,28*), only few of them have been properly screened in vivo. 2′-*O*-Alkylation of oligoribonucleotides (*29*), modifications at the base moiety structures (*30*), and freezing of the sugar ring puckering by an additional covalent bridge (*31*) have been shown to enhance the hybridization, whereas biodegradable lipophilic phosphate protective groups have been suggested to increase the cellular uptake (*32*). In practice, compromises between permeability and specificity of hybridization are inevitable. It is known that sequences of 15–20 nucleotides will enter the cytoplasm and bind mRNA (*33*). Although shorter oligonucleotides enter into the cells through the cell membrane, they may not attach strongly enough or may not be unique to bind the specific mRNA. Because the mRNA maintains a 3-dimensional structure with hairpins and bulges, we have to select a sequence that will bind without mismatch of a single base.

Other major concerns for antisense approaches are the cellular internalization and intracellular distribution; the mechanism by which oligonucleotides are taken up into cells is still poorly understood (*34*). The majority of oligonucleotides—for example, PO, PS, and OMe—are negatively charged molecules and behave as polyanions regardless of their sequence content. A hydrophilic oligonucleotide inefficiently crosses a hydrophobic cell membrane. Therefore,

several attempts have been made to enhance the cellular delivery of oligonucleotides (*35*). So far, the most commonly and successfully used delivery systems are liposomes and charged lipids, enabling internalization by endocytosis. Essentially, after reaching the endosomal compartment, the oligonucleotide must be efficiently released and set free for binding with the specific target mRNA.

In the development of new radiopharmaceuticals for PET, high specificity and high affinity of binding are important properties. Rapid localization and clearance kinetics of the tracer and its prolonged retention in the target are general requirements for nuclear imaging, whereas ribonuclease H–dependent turnover is usually desired in antisense chemotherapy. Accordingly, a particular oligonucleotide that is found to be unsuitable for antisense chemotherapy may be the molecule of choice for antisense imaging. For successful antisense imaging, target cells should have a sufficient amount of mRNA. Furthermore, the labeling of the antisense compound should not interfere with base pairing between the mRNA and the antisense molecule.

At the moment, only a few PET imaging trials with labeled oligonucleotides have been reported. Previously, Kobori et al. have successfully visualized mRNA expression in the central nervous system using PET. The PS antisense oligonucleotide for mRNA of glial fibrillary acidic protein labeled with ^{11}C was retained in tumor cells, yielding clear images of gliomas in rats (*5*). Tavitian et al. labeled PS antisense oligonucleotide with ^{18}F and performed in vivo PET studies in baboons (*10*). The study was designed only to evaluate the pharmacokinetics of the tracer, not to determine its hybridization in vivo.

The use of reporter genes instead of oligonucleotides is another alternative to in vivo imaging of gene expression. Current research in this particular field of imaging is productive. For example, PET imaging of the dopamine D$_2$ receptor in mice, using a derivative of spiperone (3-(2′-^{18}F-fluoroethyl)spiperone [^{18}F-FESP]) as a reporter gene, has been reported (*36*). Furthermore, imaging of herpes virus type 1 thymidine kinase (HSV1-tk) gene transfer and expression in vivo, using ^{124}I-5-iodo-2′-fluoro-1-β-D-arabino-furanosyluracil (^{124}I-FIAU) and PET, have been studied (*37*). Gambhir et al. used ^{18}F-fluoroganciclovir (^{18}F-FGCV) for HSV1-tk and demonstrated its accumulation in living mice with PET (*38*).

Although labeling of oligonucleotides with radionuclides is becoming fairly common, to our knowledge, radiolabeling with ^{68}Ga has not been reported by others. Considering the low abundance of mRNA targets, high specific activities of ^{68}Ga-labeled oligonucleotides are essential. In this study, the average specific activity of all ^{68}Ga labeling was 270 ± 90 MBq/mg, which converts to 1.6 ± 0.5 GBq/μmol. A specific activity of 74 MBq/mg for ^{90}Y-labeled PS oligonucleotides has been reported previously (*39*). On the other hand, compared with, for example, ^{18}F-labeled (111–195 GBq/μmol) or ^{125}I-labeled (37 GBq/μmol) oligonucleotides, the obtained specific activity is much lower (*9*). Yet,

for the present study, only 10–100 nmol of DOTA-conjugated oligonucleotide was used for the labeling reaction with [68]Ga. Our preliminary studies reveal that the radiochemical yield improves with increasing concentration of oligonucleotide, which most probably increases the specific activity also (I. Velikyan, G. Lendvai, M. Välilä, et al., unpublished data, 2003).

For in vivo antisense applications, it is important to clarify how the ^{68}Ga labeling of oligonucleotides influences their biologic properties. Our studies have revealed that the conjugate labeling with ^{68}Ga using DOTA as a chelator did not alter the hybridization or protein binding capability of the oligonucleotides. High protein binding of PS, for example, has also been reported by others (21). Furthermore, the in vitro albumin binding studies showed that the binding was clearly saturable. Such studies are relevant since the protein binding affects both tissue distribution and cellular uptake. It has been suggested that plasma proteins—for example, albumin—can act as carrier proteins and protect oligonucleotides from degradation.

The negative PCR and RT-PCR results of PS and OMe are of interest. In general, a desired PCR product is amplified if (a) the oligonucleotide primers are able to bind complementarily to the template sequence (annealing) and (b) the DNA polymerase enzyme can attach and start copying the template (extension). Our results suggest that PS and OMe are able to inhibit the primer extension most likely by directly interacting with the enzyme. Indeed, oligonucleotides carrying a PS modification are strong inhibitors of DNA polymerases in a linkage number–dependent manner. Longer oligomers are more potent inhibitors than shorter ones, and the inhibitory effect can be avoided by decreasing the number of PS linkages at the backbone. Our negative PCR results, obtained with fully thioated oligonucleotides, are in accordance with these observations. In addition, both PS and OMe oligomers can inhibit polymerization by binding to the AMV-RT rather than to the template (40).

The overall distribution of oligonucleotides relies, among other things, on protein binding in plasma and tissues, passive diffusion across the membranes, and transport into or out of the cells. The elimination kinetics in vivo of our oligonucleotides seemed to vary significantly with the nature of oligonucleotide backbone. Since these oligonucleotides did not have any biologic target in normal rats, the radioactivity distribution to various organs basically reflects their nonspecific interactions and metabolism. The biodistribution of the 3 oligonucleotides studied presumably relates to their in vivo degradation versus stability. The results obtained partially agree with those reported by Tavitian et al. on ^{18}F-oligonucleotides (10). Yet, the obvious kidney accumulation of PS is of interest. This behavior seems not to be caused by DOTA, ^{68}Ga, or the oligonucleotide sequence, but by the backbone itself. Yet, previous studies have shown that the length of PS oligonucleotides has a major impact on the body distribution pattern (7).

CONCLUSION

Our results on the biokinetics of ^{68}Ga-oligonucleotides in rats, determined using an GE Advance PET scanner, are encouraging. Intravenously injected ^{68}Ga-oligonucleotides of 17-mer length revealed high-quality PET images, allowing quantification of the biokinetics in major organs and in tumors. Further studies in a larger number of rats include clarification of the metabolic fate of ^{68}Ga-oligonucleotides in tumors and, most importantly, clarification of the in vivo specificity—that is, hybridization with the mutant K-ras mRNA—by performing comparative experiments with antisense, sense, and missense oligonucleotides. Our results show, however, that the simple and rapid ^{68}Ga labeling of oligonucleotides can be applied for PET imaging. We conclude that ^{68}Ga labeling of oligonucleotides is a convenient approach for in vivo PET imaging of the biodistribution and quantification of oligonucleotide biokinetics in living animals.

REFERENCES

1. Dewanjee MK, Ghafouripour AK, Kapadvanjwala M, et al. Noninvasive imaging of c-myc oncogene messenger RNA with indium-111-antisense probes in a mammary tumor-bearing mouse model. *J Nucl Med.* 1994;35:1054–1063.
2. Hnatowich DJ. Antisense and nuclear medicine. *J Nucl Med.* 1999;40:693–703.
3. Phelps ME. PET: the merging of biology and imaging into molecular imaging. *J Nucl Med.* 2000;41:661–681.
4. Urbain JL. Oncogenes, cancer and imaging. *J Nucl Med.* 1999;40:498–504.
5. Kobori N, Imahori Y, Mineura K, Ueda S, Fujii R. Visualization of mRNA expression in CNS using ^{11}C-labeled phosphorothioate oligodeoxynucleotide. *Neuroreport.* 1999;10:2971–2974.
6. Pan D, Gambhir SS, Toyokuni T, et al. Rapid synthesis of a 5′-fluorinated oligodeoxy-nucleotide: a model antisense probe for use in imaging with positron emission tomography (PET). *Bioorg Med Chem Lett.* 1998;8:1317–1320.
7. Wu F, Yngve U, Hedberg E, et al. Distribution of [76]Br-labeled antisense oligonucleotides of different length determined ex vivo in rats. *Eur J Pharm Sci.* 2000;10:179–186.
8. Hedberg E, Långström B. Synthesis of 4-([^{18}F]fluoromethyl)phenyl isothiocyanate and its use in labelling oligonucleotides. *Acta Chem Scand.* 1997;51:1236–1240.
9. Kühnast B, Dolle F, Terrazzino S, et al. General method to label antisense oligonucleotides with radioactive halogens for pharmacological and imaging studies. *Bioconjug Chem.* 2000;11:627–636.
10. Tavitian B, Terrazzino S, Kühnast B, et al. In vivo imaging of oligonucleotides with positron emission tomography. *Nat Med.* 1998;4:467–471.
11. Bos JL. ras oncogenes in human cancer: a review. *Cancer Res.* 1989;49:4682–4689.
12. Kahn S, Yamamoto F, Almoguera C, et al. The c-K-ras gene and human cancer (review). *Anticancer Res.* 1987;7:639–652.
13. Monia BP, Johnston JF, Ecker DJ, Zounes MA, Lima WF, Freier SM. Selective inhibition of mutant Ha-ras mRNA expression by antisense oligonucleotides. *J Biol Chem.* 1992;267:19954–19962.
14. Monia BP, Johnston JF, Sasmor H, Cummins LL. Nuclease resistance and antisense activity of modified oligonucleotides targeted to Ha-ras. *J Biol Chem.* 1996;271:14533–14540.
15. Chen G, Oh S, Monia BP, Stacey DW. Antisense oligonucleotides demonstrate

a dominant role of c-Ki-RAS proteins in regulating the proliferation of diploid human fibroblasts. *J Biol Chem.* 1996;271:28259–28265.

16. Irie A, Anderegg B, Kashani-Sabet M, et al. Therapeutic efficacy of an adenovirus-mediated anti-H-ras ribozyme in experimental bladder cancer. *Antisense Nucleic Acid Drug Dev.* 1999;9:341–349.

17. Yu RZ, Geary RS, Leeds JM, et al. Pharmacokinetics and tissue disposition in monkeys of an antisense oligonucleotide inhibitor of Ha-ras encapsulated in stealth liposomes. *Pharm Res.* 1999;16:1309–1315.

18. Cowsert LM, Ohashi CT, Bhat B, et al. MMI linkage modification increases potency and stability of H-ras antisense oligonucleotides. *Nucleosides Nucleotides.* 1999;18:1383–1384.

19. Agrawal S, Zhang X, Lu Z, et al. Absorption, tissue distribution and in vivo stability in rats of a hybrid antisense oligonucleotide following oral administration. *Biochem Pharmacol.* 1995;50:571–576.

20. Crooke ST. Proof of mechanism of antisense drugs. *Antisense Nucleic Acid Drug Dev.* 1996;6:145–147.

21. Temsamani J, Roskey A, Chaix C, Agrawal S. In vivo metabolic profile of a phosphorothioate oligodeoxyribonucleotide. *Antisense Nucleic Acid Drug Dev.* 1997;7:159–165.

22. Agrawal S, Jiang Z, Zhao Q, et al. Mixed-backbone oligonucleotides as second generation antisense oligonucleotides: in vitro and in vivo studies. *Proc Natl Acad Sci USA.* 1997;94:2620–2625.

23. Kita K, Saito S, Morioko CY, Watanabe A. Growth inhibition of human pancreatic cancer cell lines by anti-sense oligonucleotides specific to mutated K-ras genes. *Int J Cancer.* 1999;80:553–558.

24. Hermanson GT. *Bioconjugate Techniques.* London, U.K.: Academic Press, Inc.; 1996:173–176.

25. Lewis MR, Raubitschek A, Shively JE. A facile, water-soluble method for modification of proteins with DOTA: use of elevated temperature and optimized pH to achieve high specific activity and high chelate stability in radiolabeled immunoconjugates. *Bioconjug Chem.* 1996;5:565–576.

26. Dymov AM, Savostin AP. *Analytical Chemistry of Gallium.* Ann Arbor, MI: Ann Arbor Science Publishers; 1970:13–16.

27. Roivainen A, Jalava J, Pirilä L, Yli-Jama T, Tiusanen H, Toivanen P. H-ras oncogene point mutations in arthritic synovium. *Arthritis Rheum.* 1997;40:1636–1643.

28. Eckstein F. Phosphorothioate oligodeoxynucleotides: what is their origin and what is unique about them? *Antisense Nucleic Acid Drug Dev.* 2000;10:117–121.

29. Manoharan M. 2′-Carbohydrate modifications in antisense oligonucleotide therapy: importance of conformation, configuration and conjugation. *Biochim Biophys Acta.* 1999;1489:117–130.

30. Herdewijn P. Heterocyclic modifications of oligonucleotides and antisense technology. *Antisense Nucleic Acid Drug Dev.* 2000;10:297–310.

31. Kvaerno L, Wengel J. Antisense molecules and furanose conformations: is it really that simple? *Chem Commun.* 2001;5:1419–1424.

32. Bologna JC, Vives E, Imbach JL, Morvan F. Uptake and quantification of intracellular concentration of lipophilic pro-oligonucleotides in HeLa cells. *Antisense Nucleic Acid Drug Dev.* 2000;12:33–41.

33. Sazani P, Gemignani F, Kang SH, et al. Systemically delivered antisense oligomers upregulate gene expression in mouse tissues. *Nat Biotechnol.* 2002;20:1228–1233.

34. Thierry AR, Vives E, Richard JP, et al. Cellular uptake and intracellular fate of antisense oligonucleotides. *Curr Opin Mol Ther.* 2003;5:133–138.

35. Kurreck J. Antisense technologies: improvement through novel chemical modifications. *Eur J Biochem.* 2003;270:1628–1644.

36. MacLaren DC, Gambhir SS, Satyamurthy N, et al. Repetitive, non-invasive imaging of the dopamine D2 receptor as a reporter gene in living animals. *Gene Ther.* 1999;6:785–791.

37. Tjuvajev JG, Chen SH, Joshi A, et al. Imaging herpes virus thymidine kinase gene transfer and expression by positron emission tomography. *Cancer Res.* 1998;58:4333–4341.

38. Gambhir SS, Barrio JR, Phelps ME, et al. Imaging adenoviral-directed reporter gene expression in living animals with positron emission tomography. *Proc Natl Acad Sci USA.* 1999;96:2333–2338.

39. Watanabe N, Sawai H, Endo K, et al. Labeling of phosphorothioate antisense oligonucleotides with yttrium-90. *Nucl Med Biol.* 1999;26:239–243.

40. Boiziau C, Larrouy B, Sproat BS, Toulme JJ. Antisense 2′-O-alkyl oligoribonucleotides are efficient inhibitors of reverse transcription. *Nucleic Acids Res.* 1995;23:64–71.